Analysis of microstructures of laser surface-melted tool steels

P. A. MOLIAN, H. S. RAJASEKHARA
Mechanical Engineering Department, Iowa State University, Ames, Iowa 50011, USA

Several investigators [1–4] have examined the effect of laser surface melting on the microstructure, as well as the hardness, toughness, and wear properties of AISI-M2 tool steel. Their results show a considerable discrepancy in the aspect of microstructure, which may be partly due to the variations in laser parameters used. In the present work, laser glazing experiments were conducted on AISI-M2 and T1 tool steels to identify the microstructures as a function of melt depth (or cooling rate). Analysis by scanning electron microscope was employed in conjunction with X-ray diffraction to characterize the microstructures of laser-glazed surface layers. A 2.5-kW continuous-wave CO_2 laser (Photon Sources model T3000) was used in gaussian mode to melt the steels (surface-ground specimens) at speeds varying from 17 to 200 mm sec^{-1}. A single-pass melting procedure was used.

Fig. 1 shows the exponential variation of melt depth and width with scanning speed. The melt depths ranged from 50 to 1400 μm. The corresponding cooling rates were estimated to be 10^6 K sec^{-1} to 10^2 K sec^{-1} by measuring the average cellular-dendrite size and using the equation $D = 59 \times T^{-0.34}$ [1], where D is the cell size in micrometres and T is the cooling rate in K sec^{-1}. Fig. 2a to c shows the transverse sections where the melt profile changes from hourglass shape to semicircular and increases in average hardness from 580 to 700 H_v. Another interesting observation from these micrographs is the ridge at the centre and, in some cases, the crater at either end of the melt zone. This is due to the difference in surface tension between the centre and edge of the melt pool, to the carryover of some molten metal along its motion by the beam, and to the "keyhole" phenomenon. Fig. 3a to c shows optical micrographs showing the increase in fineness of cellular-dendrite structures with a decrease in melt depth.

Fig. 4 is a representative scanning electron micrograph of the melt zones indicating the absence of coarse carbide formation. X-ray powder diffraction patterns, taken from three melt zones (Fig. 2), revealed that the microstructures were essentially a mixture of martensite (bct), δ-ferrite (bcc), $M_{23}C_6$ carbide, and some retained austenite. The proportions of δ-ferrite were increased at the expense of martensite, when melt depth was reduced. In short, the shallow melt zone exhibited δ-ferrite cells and peritectic $\gamma/M_{23}C_6$ at the cell boundaries, whereas the deep melt zone contained martensite cells with the cell boundaries enriched with retained austenite and $M_{23}C_6$ carbide.

Figs 5 and 6 provide the variation of hardness with scanning speed and depth below the surface. It is evident that hardness was increased as melt depth decreased and that higher hardness is always obtained near the surface as opposed to the bottom of the melt zone. The hardness data coupled with microstructural observations suggest that δ-ferrite cells had a higher hardness than martensite cells. This is rather surprising but is attributed to the following reasons: (i) δ-ferrite cells are much finer than martensite cells; (ii) dislocation density of δ-ferrite may be high; (iii)

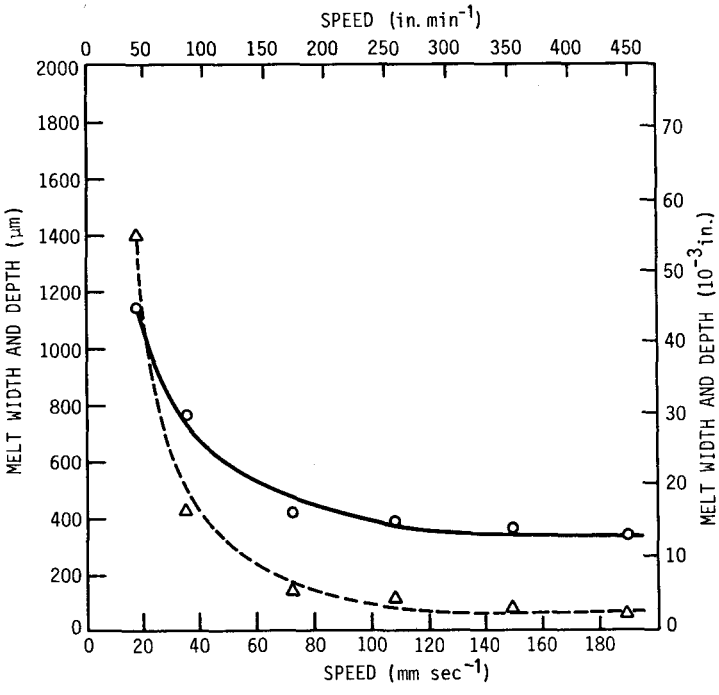

Figure 1 Effect of beam traverse speed on the depth (△) and width (○) of melt zone. Material: T1 tool steel. Laser: 2.5 kW, gaussian, focused on surface.

0261–8028/86 $03.00 + .12

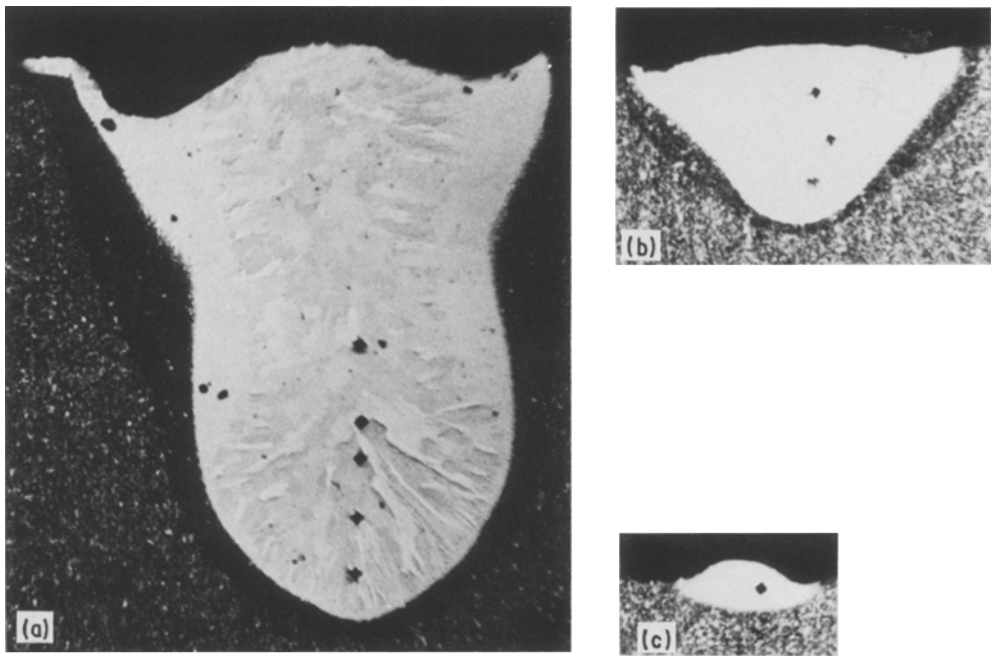

Figure 2 Transverse sections of laser-melted T1 tool steel as a function of beam traverse speed: (a) 17 mm sec^{-1}, (b) 35 mm sec^{-1}, (c) 110 mm sec^{-1}. × 50. Note the Vicker's microhardness indentations.

δ-ferrite may be highly supersaturated with chromium, tungsten and molybdenum; (iv) $M_{23}C_6$ carbide may be finer at the cell boundaries of δ-ferrite than in martensite because of cooling rate differences.

Ahman [1] observed martensite cells (1.5 to 2 μm) in laser-melted M2 tool steel for a melt depth of 950 μm. Furthermore, transmission electron microscopy analysis of laser-glazed layers by Ahman [1] did not reveal any evidence of carbide formation. This intriguing feature is in contradiction with the results obtained in this work and elsewhere. Other investigators [2–4] generally agree that laser melting results in complete dissolution of metal carbides and inceases the carbon and alloy content of the matrix. During the subsequent solidification, precipitation of carbide occurs on an ultrafine scale. Ahman argued that solidification cooling rate is quite high (4×10^4 K sec^{-1}) to allow the carbide to form.

Strutt *et al.* [2, 3] characterized the microstructures of laser-melted M2 steel for a melt depth of 250 μm. The microstructure near the top of the melt zone consisted of δ-ferrite cells with boundaries containing retained γ, M_2C, and $M_{23}C_6$ carbides; the microstructure yielded a hardness of 650 H_v. In contrast, the bottom of the melt zone exhibited a completely austenite structure with a hardness of 950 H_v. Strutt *et al.* [2] believed that the peritectic reaction $\delta + L \rightarrow \gamma + M_{23}C_6$ did not go to completion near the surface because of the high freezing rate that drastically reduced the redistribution of alloying elements by diffusion. They also claimed that the slow velocity of the liquid to solid interface was responsible for the presence of austenite at the bottom of the melt zone.

Kear *et al.* [4] investigated the microstructure and hardness of laser-glazed tool steels such as 440 C and M2. The melt zone of alloy 440 C exhibited δ-ferrite

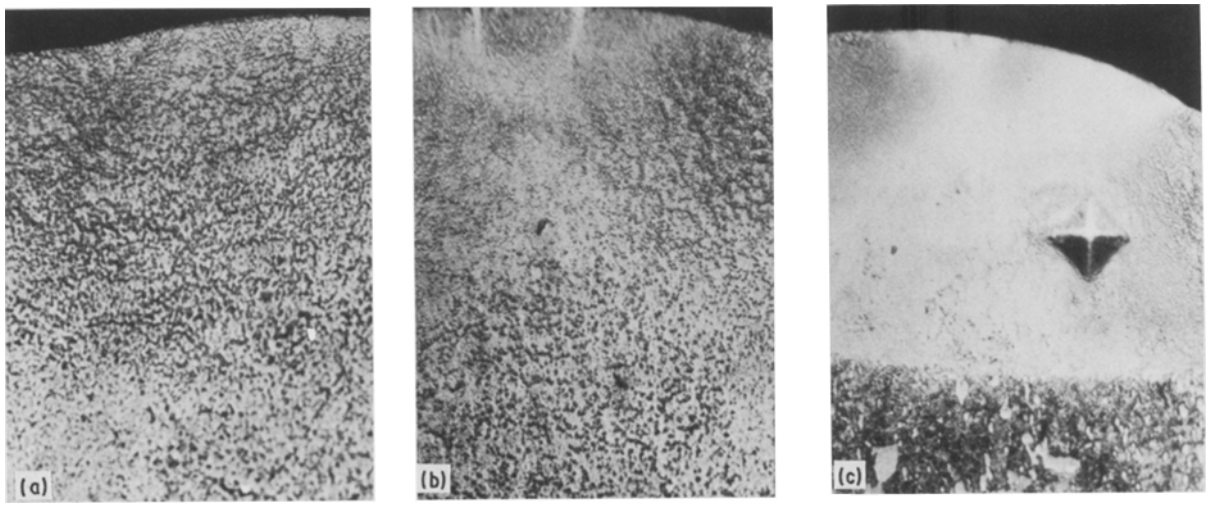

Figure 3 Light micrographs of the microstructure of melt zones obtained at different beam traverse speeds: (a) 17 mm sec^{-1}, (b) 35 mm sec^{-1}, (c) 110 mm sec^{-1}. × 400

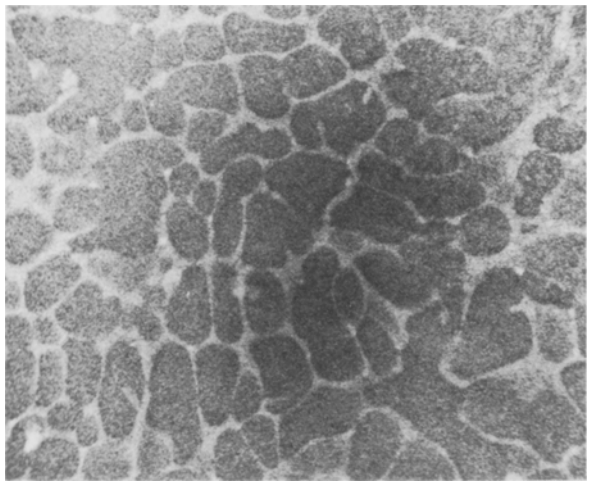

Figure 4 Scanning electron micrograph of laser-melted tool steel processed at a speed of 17 mm sec^{-1}. × 6500

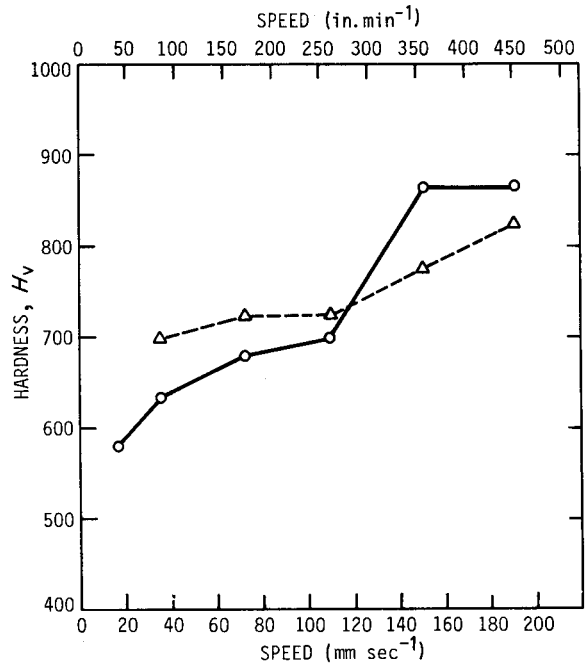

Figure 5 Variation of a melt zone hardness with beam traverse speed. Materials: T1 (○); M2 (△).

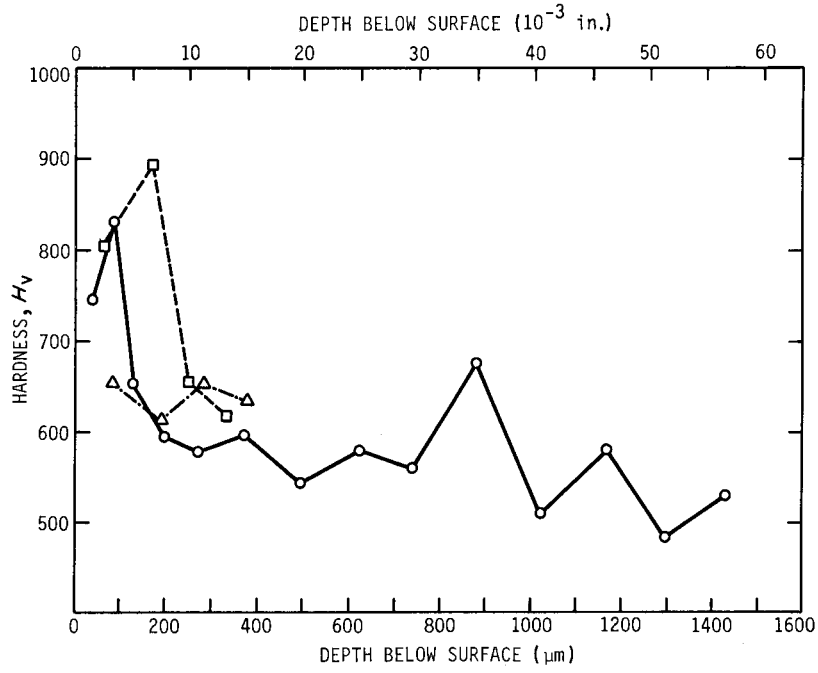

Figure 6 Hardness variations along the melt depths. Materials: (○) T1 (17 mm sec^{-1}); (△) T1 (35 mm sec^{-1}); (□) M2 (35 mm sec^{-1}).

dendritic structure, interspersed with thin sheets of carbide in the interdendritic regions. The hardness of the melt zone was 470 H_v. In contrast to alloy 440 C, the laser melt zone of alloy, M2 showed no indication of dendritic structure. The melt zone had a hardness of 600 H_v and was composed of δ-ferrite/γ structures.

From the foregoing results and discussion, it appears that the microstructure of laser-glazed tool steels (for shallow melt depths) is essentially a mixture of δ-ferrite, fine carbides, and austenite. The transition from δ-ferrite to martensite with an increase in melt depth occurs because of the slower cooling rate that causes the peritectic reaction to occur and thereby results in the transformation of austenite to martensite.

Acknowledgements

We thank the Iowa High Technology Council and the State of Iowa for financial support, and also Photon Sources, Livonia, Michigan, for the use of their laser facility.

References

1. L. AHMAN, *Metall. Trans.* **15A** (1984) 1829.
2. P. R. STRUTT, M. TULI, M. NOWOTNY and B. K. KEAR, *Mater. Sci. Engng* **36** (1978) 217.
3. P. R. STRUTT, *Mater. Sci. Engng J.* **44** (1980) 239.
4. B. H. KEAR, E. M. BREINAN and L. E. GREENWALD, *Metals Technol.* **6** (1978) 121.

Received 7 April
and accepted 8 May 1986